Liu, S., Cao, Q., Zhao, X., Lu, Z., Deng, Z., Dong, J., Lin, X., Qing, K., Zhang, W., and Chen, Q. 2020. "Improving indoor air quality and thermal comfort in residential kitchens with a new ventilation system," *Building and Environment*, 180:107016.

Improving indoor air quality and thermal comfort in residential kitchens with a new ventilation system

Sumei Liu[a,b], Qing Cao[c], Xingwang Zhao[a,b], Zechao Lu[b], Zhipeng Deng[b], Jiankai Dong[d,e*], Xiaorui Lin[f], Ke Qing[f], Weizhen Zhang[f], Qingyan Chen[b]

[a]*Tianjin Key Laboratory of Indoor Air Environmental Quality Control, School of Environmental Science and Engineering, Tianjin University, Tianjin, China*

[b]*School of Mechanical Engineering, Purdue University, West Lafayette, IN, USA*

[c]*School of Civil Engineering, Dalian University of Technology, Dalian, China*

[d]*School of Architecture, Harbin Institute of Technology, Heilongjiang Province, 150006, China*

[e]*Key Laboratory of Cold Region Urban and Rural Human Settlement Environment Science and Technology, Ministry of Industry and Information Technology, China*

[f]*Vanke Real Estate Development Co. Ltd., Changsha Vanke, Hunan Province, 410000, China*

**Corresponding email: djkheb@163.com*

ABSTRACT

Chinese kitchen environment is usually hot and humid in summer and cold in winter, while people spends considerable time there. This investigation firstly assessed the indoor air quality and thermal environment in a kitchen in summer in Changsha, China. Sixteen cooks were asked to prepare the same dishes in the kitchen. The study measured skin temperatures of the cooks and environmental parameters (air temperature, CO, CO_2, TVOCs, and $PM_{2.5}$) and recorded their thermal sensation votes using questionnaires at the same time. The results show that the thermal environment in the kitchen was highly non-uniform and too hot in summer. The air temperature in the kitchen could increase 5.3°C during cooking. TVOCs and $PM_{2.5}$ concentrations exceeded the limits by Chinese standards in the kitchen. Thus, this investigation proposed a new ventilation system to improve the indoor environment in Chinese residential kitchens. The new ventilation system had upward air curtains around the gas stove and conditioned air from the cabinet under the stove. A systematic numerical study using the steady state RNG k-ε model was performed to optimize the integrated system design for both summer and winter conditions. Experimental measurements were conducted in a kitchen mockup to verify the performance of the new system. The measured capture efficiency of the new system was 96.2% to 97.1%, the predicted dissatisfied percentage (PD) distribution around the cook smaller than 20%, and the vertical temperature difference between head and feet -0.9°C.

Keywords: Thermal comfort, Indoor air quality, RNG k-ε model, Air conditioning, CFD

HIGHLIGHTS

- Thermal comfort level and IAQ were poor in Chinese residential kitchen
- Proposed of an integrated air curtain and air-conditioning system to improve thermal comfort and IAQ in residential kitchens

- Optimization of the new ventilation system by means of CFD simulations
- Verification of the computed results with corresponding experimental data

1. Introduction

As an important daily activity, household heads spend about 3.6 hours per day in residential kitchens [1,2], and thus a healthy and thermally comfortable kitchen environment is essential. However, the indoor environment in Chinese residential kitchens (CRKs) is not satisfactory. Epidemiological evidence has confirmed an association between exposure to cooking fumes and lung cancer risk among never-smoking women in China, especially in poorly ventilated settings [3,4,5]. A recent survey [6] revealed that 89% of respondents complained about exposure to kitchen fumes.

There are two main reasons for these complaints. First, the thermal environment in CRKs is unfavorable [7,8]. Similarly, Wei et al. [2] found that the vertical temperature difference could reach 6.3°C, which exceeded the maximum difference of 3.0°C accepted for thermal comfort [9]. Zhou et al. [10] conducted human subject tests for 20 cooks as they prepared dishes in a CRK under summer conditions. The researchers found that the subjects' thermal sensations (TSV) increased by 0.5 units when the stove was turned on. After 15 minutes, the median TSV reached the highest level of +3 (very hot). The second reason for dissatisfaction is the extremely poor indoor air quality (IAQ) in Chinese residential kitchens [11]. According to data from the literature [12,13], most CRKs were found to have gaseous air pollutants (such as CO, CO_2, NO_2, and TVOCs (total volatile organic compounds)) and particulate matter that exceeded the limits set by the Chinese national standard [14]. Some kitchens had excessively high pollutant concentrations [15,16], which could exceed the limits in the national standard by more than 10 times. Many studies [17,18] have demonstrated that air pollutants are harmful to human health. Overall, most Chinese residential kitchens exhibit thermal discomfort and poor indoor air quality. Therefore, it is important to improve indoor air quality and thermal environment in CRKs.

Exhaust hood was generally used to extract cooking generated pollutants and waste heat to outdoor space for improving indoor air quality and thermal environment in CRKs. The suggested exhaust airflow rate in CRKs should not be smaller than 600 m^3/h [19] when the hood is operating at the highest speed, which corresponds to an air change rate of 50 h^{-1} in a kitchen with a floor area of 4 m^2 and height of 3 m. Since most CRKs had only a simple exhaust hood and did not have air conditioning or make-up air systems, the make-up air for the exhaust hood must come from an opened window/door and cracks. However, most of Chinese residents closed their windows and doors during cooking due to unfavorable outdoor weather conditions, and cooking fumes as well as noise generated during cooking [6,15]. The median infiltration rate was only 0.37 h^{-1} in northern China and 0.42 h^{-1} in southern China according to the measurements from Liu et al. [20]. Under such airtightness, even if the kitchen door was open, the airflow from the living room would be too low to provide enough make-up air. If the window is open to provide make-up air, it will lead to an excessively hot thermal environment in summer and cold thermal environment in winter. In addition, airflow from the window would cause an obvious disturbance of the air distribution around the stove region, which would bring negative effects on the performance of the exhaust hood [21].The use of a range hood with uncontrolled natural ventilation would be challenging for removal of cooking pollutants. Therefore, it is important to explore how to provide reasonable make-up air and conditioned air in CRKs to improve the kitchen environment.

Unlike commercial kitchens, most CRKs had only a simple exhaust hood and did not have air conditioning or make-up air systems. Some investigators have used downward [6,22] or

upward [6,21,23,24,25] plane jets to form air curtains around stove to restrain the spillage and provide make-up air for the exhaust hoods in CRKs. However, the airflow rate supplied from the curtains in the previous investigations accounted for less than 30% of the exhaust hood airflow rate. Most of the make-up air had to come from window, door or leakages. However, it is not practical to open window when outdoor is too hot in summer, too cold in winter or outdoor air quality was poor. In addition, the current airtightness made it difficult to provide enough make-up air from the leakage for the exhaust hood. Thus, the use of previous air curtains would potentially improve IAQ in CRKs but could not solve the problem completely, especially for the indoor thermal environment.

Commercial kitchens use air conditioning to create a thermally comfortable environment [26]. Many air-conditioner manufacturers have pushed very hard by advertising for the use of their appliances in CRKs. The use of air conditioners in CRKs seems like a good idea to improve indoor thermal comfort for CRKs, but our literature search did not find many studies on the subject. Without using a make-up air system, the supply air from the conditioner may disturb the air distribution around stove, and thus decrease the capture efficiency of exhaust hood. In addition, the conditioned air in the kitchen was discharged directly to outdoor environment by the exhaust hood, which would lead to energy waste. Such system could not prevent cooking fume from entering the kitchen air so particles could deposit on walls and other kitchen surfaces. Furthermore, conditioned air may interact with airflow from the make-up air systems and the airflow to the exhaust hood. Huang et al. [27] found that exhaust hood performance was very sensitive to local drafts. Therefore, systematic study for identification of the best air conditioner and makeup air system with optimal air supply parameters was needed under both summer and winter conditions.

This paper reports our effort in designing a new ventilation system to improve the environment inside CRKs. Our goal was to propose a suitable ventilation system to solve the problem of thermal discomfort and poor IAQ in CRKs. We performed a systematic study to optimize the proposed system.

2. Research Method

2.1 Thermal comfort and indoor air quality in Chinese residential kitchen

In order to better understand the thermal environment and indoor air quality inside CRKs, we conducted experimental tests in a CRK in late summer (September 13 to 14, 2018) in Changsha, China, which belongs to the subtropical monsoon climate. Fig. 1(a) shows the kitchen was 2.9 m long, 1.85 m wide, and 2.3 m high. The vent from the side of the exhaust hood shown in Fig. 1(b) was designed to supply makeup air for the hood of another system. It did not run during our experiment. Sixteen subjects, nine males and seven females with an average age of 22 (standard deviation = 4) from a cooking school, participated in the tests. Previous investigation [28] found that cooking method was the most important factor for cooking emissions, and stir-frying released the greatest number of cooking pollutants. In addition, 84.6% of Chinese people prefer stir-frying when they are cooking at home [29]. Therefore, this investigation asked the subjects to cook two dishes (one capsicum-fried meat firstly and the other stir-fried vegetables secondly) in the kitchen during the experiment. We mainly focused on the overall influence on environmental parameter variations and the thermal comfort of the subject due to the real cooking period. Therefore, the order of the two dished should have little influence on the overall effect. These two dishes were the typical Hunan cuisines. The total cooking period lasted around 20 to 30 minutes, including washing, cutting, and stir-frying etc. The pure stir-frying period for both dishes lasted for 3 to 5 minutes. This investigation measured cooks' skin temperature (Tsk) and environmental parameters and

recorded their thermal sensation votes (TSV) by using subjective questionnaire survey. We also measured air quality in the kitchen at the same time.

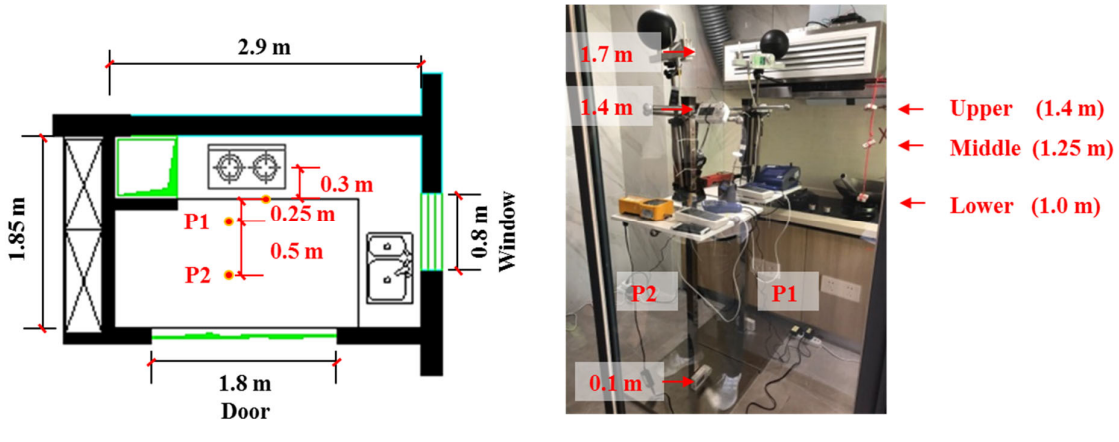

(a) (b)

Fig. 1. Experimental setup in a kitchen thermal environment measurements. (a) Plan view of the kitchen, and (b) the actual kitchen layout. HOBO data loggers were hung on poles P1 and P2 at heights of 0.1, 1.4, and 1.7 m above the floor in the occupied zone of the kitchen.

We used nine HOBO U12-013 loggers from ONSET to record the air temperature in the kitchen, at heights of 0.1, 1.4, and 1.7 m above the floor in P1 and P2 poles and at three locations (upper, middle, and lower) between the gas stove and the hood as shown in Fig 1. We also used one HOBO logger to measure outdoor air temperature and humidity. The HOBO loggers had a measuring accuracy of ±0.2ºC for air temperature. The measuring frequency was every minute. We started the HOBO loggers before the experiment began and collected the data after the experiment finished. All the instruments were started using the same computer. Thus, it could maintain the synchronisation of all instruments with time log.

This study also measured the indoor air pollutant concentrations during cooking. A HOBO MX1102 logger was used to measure CO_2 concentration in the kitchen with an accuracy of ±50 ppm. A TSI IAQ CALCTM 7574 was used for measuring CO concentration with an accuracy of ±3.0%. Measuring frequency for CO and CO_2 was every minute. The measured data was averaged for the whole cooking period. In order to measure TVOC concentration, Tenax TA tubes were used for sampling air at 0.4 L/min for 5 min. Each sampling started when the subject added cooking material into the pan and started to stir-fry. The analysis of TVOCs used thermal desorption gas chromatography mass spectrometry (TD-GCMS). This investigation also used a TSI DustTrack 8533 to measure the $PM_{2.5}$ mass concentration. All measuring instruments were placed on a table at 1.4 m above the floor in position P1.

This investigation studied the impact of kitchen thermal environment on the subjects by subjective questionnaires survey for recording the thermal sensation votes from the subjects. The kitchen door was glazed door. We asked the subjects to vote their thermal sensations every minute during cooking. We then recorded their TSV manually by our experimenter standing outside the glazed door of the kitchen. All the subjects wore typical summer clothing, which is a combination of short sleeve, pants, underwear, socks, and sneaker, with a clothing thermal resistance of 0.56 clo. At the same time, this study measured the skin temperatures (T_{sk}) of the subjects. Previous investigations [21,30,31] used different measuring points varied from 10 to 16 locations. During the cooking process, the upper front of the cook's body will be directly affected by the stove. Therefore, we put more measuring locations on these regions including left and right body parts. The stove has little influence on the lower and back of the body, therefore, we used single measuring point for these body parts. The total measuring points was

18. The skin temperature was measured with wireless button thermometers (DS1923-F5# iButton) [2]. The wireless button thermometers had a measuring accuracy of ±0.5°C. The measuring frequency was every 5 seconds. The measured data was averaged every minute to be consistent with the TSV data. Fig. 2 depicts the skin temperature measurement locations.

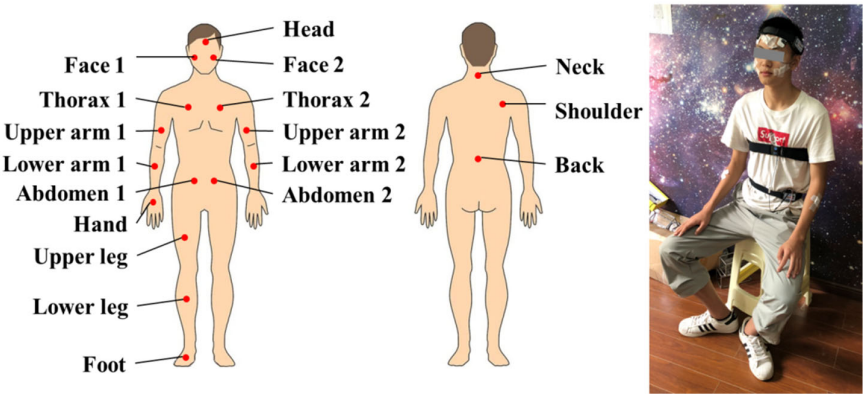

(a) (b)

Fig. 2. Measurement positions for skin temperature: (a) schematic view and (b) a subject wearing wireless button thermometers.

The experimental process was as follows: Before each test, the external window and interior door were opened. A portable vertical fan in the kitchen and the exhaust hood were turned on about 20 minutes and then the window and door of the kitchen were closed for 10 minutes. The effort was to ensure the kitchen started with a non-conditioned status as most CRKs. At the same time, we asked the subject to stay at a preparation room with an ambient temperature close to 26°C for at least 30 minutes to achieve a neutral thermal state. During their stay in the room, all the subjects were briefed on the experimental procedure and taped the wireless button thermometers on their skin. At the same time, we recorded their TSV every minute. After they reached the thermal neutral status for at least 5 minutes they went to the kitchen and the exhaust hood and the stove were switched on. The external window and door were closed during cooking. The total cooking period lasted around 20 to 30 minutes. During this time, we asked the subjects to vote their thermal sensations every minute. When the cooking was finished, the subject left the kitchen. Each test took 50 to 60 minutes depending on the cooking speed.

The purpose of our field experiment is to better understand the current status of the indoor environment inside CRKs. Therefore, our measurements only recorded the spatial distributions and variations of the environmental parameters in the kitchen.

2.2 Proposed new integrated air curtains and air-conditioning system

In order to improve the thermal environment and IAQ in kitchens, this investigation proposed an integrated air curtains and air-conditioning system to organize make-up air and conditioned air for CRKs. The system supplied conditioned air from the lower part of cabinet under the cooking stove and untreated outdoor makeup air from the two sides and the front edge of the stove. The cook fume was exhausted from the hood above the stove. Since the fumes from cooking would adhere on the surface of air vents and further affect the heat transfer if the return air is from kitchen space directly, therefore, it was best to operate the air conditioner with 100% fresh air. The system was inspired by previous research findings that locally personalized ventilation [32,33] and task air-conditioning [34,35] can thermally satisfy human's thermal comfort within a much wider room air temperature range, resulting great

potential of energy saving [36]. And the utilization of air curtain could increase the exhaust performance for pollutant and heat [21,23]. Fig. 3 shows the ventilation system diagram.

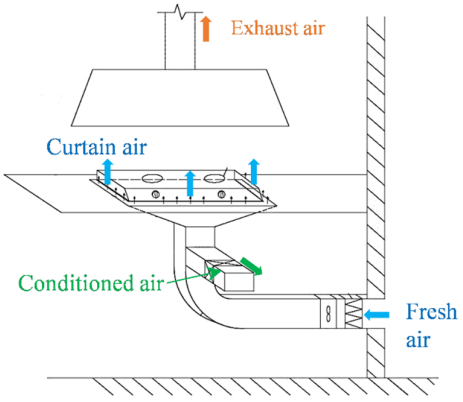

Fig. 3. The ventilation system principle diagram

Fig. 4 is a schematic of the new ventilation system developed by this investigation. According to Liu et al. [37], we used a typical Chinses kitchen layout to conduct the numerical optimization for the new ventilation system. We used the same boundary conditions to conduct the systematic design. The simulation scenario was ideal condition instead of actual cooking process. Therefore, we did not maintain every detail the same with that of the field measurement. In addition, we constructed a mockup exactly the same size and layout in an environmental chamber at Purdue University in the United States to verify the performance of the new system. The system used upward air curtains around the gas stove and conditioned air from the cabinet under the cooking stove. The ventilation system used the conditioned air and air curtains as the make-up air for the exhaust hood. The air curtains were designed to prevent spillage of cooking fumes from stove to kitchen. The air conditioner was used to heat or cool the kitchen air for thermal comfort, while the exhaust hood extracted contaminated air to the outside. The purpose of the design was to separate the air curtains from the conditioned air.

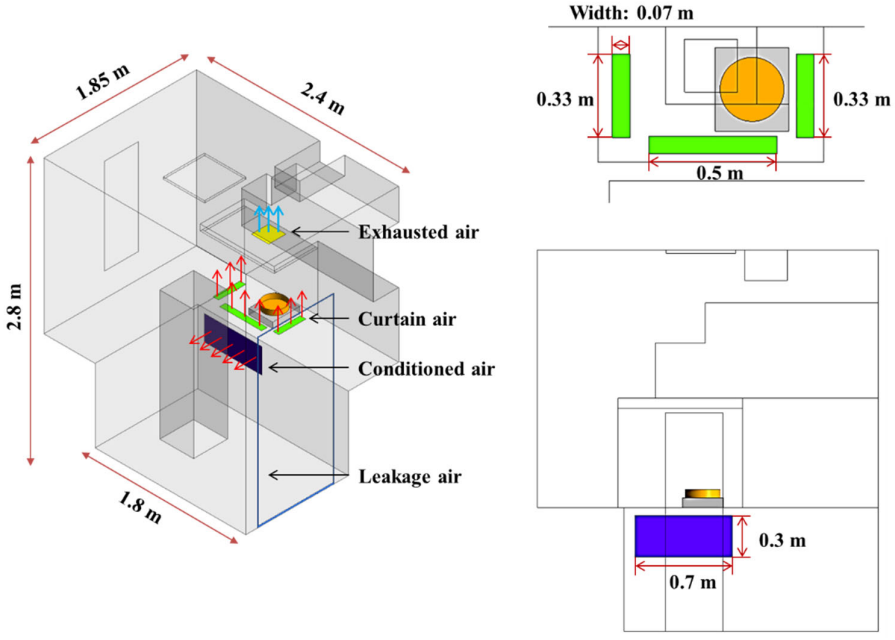

Fig. 4. Schematic of the new ventilation system

To evaluate the performance of the new ventilation system in providing thermal comfort in CRKs, this investigation used the predicted dissatisfied percentage (PD) due to draft [38] and the vertical temperature difference (ΔT) [9]. These indices were widely used in previous investigations [2,21,27] to evaluate the thermal environment inside the kitchen. PD was calculated according to equation (1). Strictly speaking, PD reflects the local-body sensation of a person. Since we had air velocity and temperature information for every point in the kitchen, we could determine the PD distribution around a human body. The PD distribution domain was set as the area 0.1 m away from the cook. This distribution may not be the actual sensation, but rather the degree of draft. According to the ASHRAE Standard 55-2010 [9], the PD around the cook should be smaller than 20%, and ΔT lower than 3.0°C.

$$PD = (3.143 + 0.3696vT_u)(34 - T_a)(v - 0.05)^{0.6223} \quad (1)$$

where PD is the percentage of people dissatisfied due to draft (%), v air velocity (m/s), T_u turbulence intensity (%), and T_a air temperature (°C).

To evaluate indoor air quality, this study used the capture efficiency (*CE*) [39], which was calculated by

$$CE = {}^{N_{outlet}}/_{N_{total}} \quad (2)$$

where *CE* is the capture efficiency, N_{outlet} the particle number at the hood exhaust, and N_{total} the total particle number emitted during cooking. Previous investigations found that considerable $PM_{2.5}$ was emitted during cooking processes [40,41]. Therefore, we used the $PM_{2.5}$ number concentration to calculate the capture efficiency.

2.2.1 Systematic parameter studies for the new ventilation system

This investigation designed a systematic study to optimize the integrated system design for both summer and winter conditions. Table 1 shows the airflow rate and air temperature from different ventilation components of the new system. The airflow rate of the hood was set according to our measurements in the laboratory. Although the nominal airflow rate of the hood was 1050 m^3/h, the measured airflow rate was only 750 m^3/h. This is mainly due to high resistance in duct found in most Chinese kitchens. The airflow rate from the air conditioner was set according to our online survey. We searched kitchen air conditioner from electronic business platform. The cooling capacity of kitchen air conditioners available ranged from 2.5 KW to 7.0 KW. By using 250 m^3/h air flow rate and the season average design weather data from Changsha, the cooling capacity was 3.8 KW. The airflow rate for the air curtains was set as 450 m^3/h, which accounts for 60% of the total airflow rate of the exhaust hood. In order to keep the kitchen under slightly negative pressure, we assumed the infiltration from the doors to be 50 m^3/h. In fact, infiltration could come from any leak from the whole kitchen. It is challenging to obtain the actual infiltration location and infiltration rate. It is also difficult to deal with the grid in those regions. Therefore, this investigation assumed all infiltration came from door leakage, as shown in Fig. 4. The width of the leakage was 0.05 m. The corresponding air velocity from the leakage was 0.21 m/s, which would have little influence on the main air flow pattern in the kitchen. In addition, we assumed a worst scenario that the air temperature from the infiltration is the untreated outdoor air, as shown in Table 1. The make-up air from the air curtains was untreated outdoor air. This investigation used season average design weather data from Changsha, China [42], for the summer and winter conditions.

The airflow rate and air temperature from different ventilation components were set according to Table 1. For the human body, a constant surface temperature of 30°C recommended by Gao and Niu [43] was adopted. The human body was a box with dimensions of 0.41 m × 0.41 m × 1.68 m to simulating a standing person. The distance between the human body and the cooking table during cooking processes was 0.35 m. The center of the human body was aligned with the center of the stove. Previous investigations [6,22,44] used non-slip wall boundary conditions with assigned wall temperature to simulate the cooking process in CRKs. This study placed a pan with a diameter of 0.25 m and a height of 0.06 m on top of a range as shown in Fig. 4. The pan bottom was heated to 310°C and the pan wall to 120°C. This thermal condition should be close to typical frying process in Chinese cooking and were also the same as those used by Cao et al. [6].

Table 1. Airflow rate and temperature for the new ventilation system

	Flow rate (m^3/h)	Temperature (°C)	
		Summer	Winter
Exhaust hood	750	--	--
Make-up air through air curtains	450	35.8	-1.9
Conditioned air	250	21	24
Infiltration from door leakage	50	35.8	-1.9

The new system supplied conditioned air from the lower part of the cabinet. Since the air supply inlet was close to the cook, it could have created draft and a large air temperature difference. Therefore, this investigation first evaluated the influence of air supply direction on the thermal comfort of the cook. To prevent draft, the conditioned air was supplied upward in summer and downward in winter. As shown in Table 2, Cases 1s to 3s were designed for studying different air supply angles from the air conditioner, Cases 3s to 5s for different air supply angles from the air curtains, and Cases 3s, 6s and 7s for different air supply velocities from the air curtains. All these cases represented summer conditions. Cases 1w to 7w represented winter conditions. Fig. 5 shows the various air supply angles and velocities for the new system.

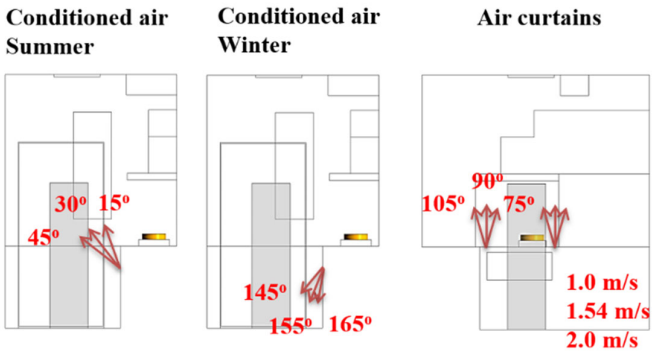

Fig. 5. Different air supply angles and velocities for the new ventilation system.

Table 2. Case setup for the new ventilation system

		Conditioned air				Air curtain			
Season	Case	T (°C)	Angle (°)	V (m/s)	Q (m^3/h)	T (°C)	Angle (°)	V (m/s)	Q (m^3/h)
Summer	1s	21	45	0.47	250	35.8	90	1.54	450
	2s	21	30	0.66	250	35.8	90	1.54	450
	3s	21	15	1.28	250	35.8	90	1.54	450
	4s	21	15	1.28	250	35.8	75	1.54	450
	5s	21	15	1.28	250	35.8	105	1.54	450
	6s	21	15	1.28	250	35.8	90	1.0	450
	7s	21	15	1.28	250	35.8	90	2.0	450
Winter	1w	24	145	0.58	250	-1.9	90	1.54	450
	2w	24	155	0.78	250	-1.9	90	1.54	450
	3w	24	165	1.28	250	-1.9	90	1.54	450
	4w	24	155	0.78	250	-1.9	75	1.54	450
	5w	24	155	0.78	250	-1.9	105	1.54	450
	6w	24	155	0.78	250	-1.9	90	1.0	450
	7w	24	155	0.78	250	-1.9	90	2.0	450

2.2.2 Numerical procedure

This investigation used a commercial CFD program, ANSYS Fluent 14.0 [45], to evaluate the performance of the new ventilation system. The evaluation used steady-state Reynolds-averaged Navier-Stokes (RANS) equations with the RNG k-ε turbulence model [46] to solve the airflow and temperature fields in the kitchen. The governing transport equations were solved by means of the finite volume method. The numerical method used the SIMPLE algorithm for coupling pressure and velocity equations, and the second-order discretization schemes for the convection and viscous terms of the governing equations. The results were considered converged when the residuals for all the independent parameters reached 10^{-4}.

This investigation evaluated indoor air quality by using the Lagrangian method to track individual $PM_{2.5}$ particle (oil mist) motion based on the airflow distribution calculated from CFD. The turbulent flow field is treated as a continuous phase and simulated in the Eulerian frame. Previous investigation [47] found that the pressure gradient force and the virtual mass force could be neglected due to small ratio of air density to particle density. The Saffman's force and Brownian force only have effect on sub-micron particles [48]. Considering the small amount of the aerosol particles in indoor air, the collision in particles can be neglected [49,50]. Therefore, this investigation did not consider them in the particle movement equation. The Lagrangian method determines the particle model in accordance with Newton's law:

$$\frac{du_p}{dt} = \frac{18\mu_a}{\rho_p d_p^2 C_c}\left(u_a - u_p\right) + \frac{g(\rho_p - \rho_a)}{\rho_p} \quad (3)$$

where the first and second terms on the right-hand side represent the drag force and gravity term, respectively, μ_a air viscosity, d_p particle diameter, u_p particle velocity, u_a air velocity, g gravitational acceleration, ρ_p particle density, ρ_a air density, and C_c the Cunningham correction factor. The factor can be expressed as:

$$C_c = 1 + \frac{2\lambda}{d_p}(1.257 + 0.4\exp(-1.1d_p/2\lambda) \quad (4)$$

where λ is the mean free path of air molecules.

Particle turbulent dispersion, which is associated with instantaneous flow fluctuations, is one of the main mechanisms of particle spreading. This study used the discrete random walk (DRW) model to calculate the particle turbulent dispersion. One-way coupling was used to simulate the interaction between the airflow and particles. The particle density was 950 kg/m^3. This study released the monodisperse spherical particles into a pan on the stove. To obtain a statistically independent result for particle deposition, we released a total of 2.4 million spherical particles into the pan uniformly with an initial velocity of 0.1 m/s. The velocity direction is normal to the bottom of the pan.

This study assumed no particle resuspension, so particles were trapped once they reached a wall surface. When a particle passed through the hood exhaust, the calculation of the particle trajectory ended. Chen et al. [51], found that four-time constants would provide consistent and accurate results. Therefore, this study performed the calculation for four-time constants of the kitchen to obtain the particle deposition results. For more detailed information about the numerical technique, please refer to the ANSYS Fluent manual [45].

Gambit software (version 2.4.6) [52] was used to generate a discrete grid for discretizing the governing transport equations. Because of the complexity of the geometrical model, this study used the tetrahedral grid scheme, which can be adapted to various geometric structures. We tested grids with 0.5, 1.4 and 3.6 million cells. It can be found that the grid number of 1.4 million provided grid-independent results. The grid size for 1.4 million cells ranged from 0.01 to 0.03 m, depending on the geometric requirements. The average wall y+ was 18, and thus the standard wall functions could be used. More detailed information about the grid analysis can be found in Appendix 1.

2.3 Experimental measurement verification for the new ventilation system

For verification of our CFD simulation results, experimental measurements with the new ventilation system were conducted in a kitchen mockup at Purdue University. Fig. 6 is a photograph of the kitchen mockup for the new ventilation system. The kitchen mockup was built in a well-insulated chamber with separate air-handling systems, one system to provide conditioned air and another to provide outdoor air. The systems include a chiller unit, a condensing unit, two heaters, two variable fans. The temperature and air flow rate are controlled in both systems by the Modular Building Controller (MBC), the central monitoring and control system. With the use of control system, the supply-air flow rate and temperature could be adjusted as needed. The block column was a box with dimensions of 0.41 m × 0.41 m × 1.68 m simulating a standing person, heated internally by a 261 W power source to simulate a standing cook. Five omnidirectional anemometers were used to measure the air velocity and temperature in the kitchen. The anemometers can measure air velocity between 0.05 and 5 m/s with a reading accuracy of 0.01 m/s, and air temperature between 0 and 60^{o}C with a reading accuracy of 0.5^{o}C. A portable data logger connected to the anemometer recorded the data at 1 Hz frequency. The data was averaged over a period of 30 to 50 min for further

analysis. Previous investigations [53,54,55] found that $PM_{2.5}$ followed the airflow very closely, just as a gas would. Tang et al. [56] reported that airborne particles smaller than 5-10 μm can be simulated with tracer gas, as they often stay suspended in the air for long time. Noakes et al. [57] found good agreement between the flow behavior of N_2O tracer gas and 3-5 μm particles in indoor environment. Bivolarova et al. [58] found that the N_2O tracer gas and 3.5 μm particles followed identical patterns at the measuring points with only 2%-9% difference between the normalized concentrations. Therefore, this investigation used sulfur hexafluoride (SF_6) as the tracer gas for $PM_{2.5}$. The measurement for capture efficiency followed the procedure of the ASTM standard [59,60], where the CE for tracer gas was determined by

$$CE = \frac{C_e - C_c}{C_e - C_a} \tag{5}$$

where C_e is the SF_6 concentration at the hood exhaust (ppm), C_c is the SF_6 concentration at selected location inside the kitchen (ppm) according to the ASTM standard [59] as shown in Fig. 6, and C_a is the ambient SF_6 concentration (ppm).

The SF_6 concentration in the kitchen mockup was sampled by a multi-point sampler [61] and analyzed by a photoacoustic multi-gas analyzer [62]. According to manual of our multi-gas analyzer, the detection limit for 0.5 s measurement is 0.019 ppm and for 50 s measurement 0.002 ppm. Due to a shortcut in our lab, we actually measured a SF_6 concentration of 0.06 ppm from the supply air. Thus, the measured data in the kitchen was always higher than 0.06 ppm. The experiment released a source contained 1% of SF_6 at a rate of 350 cm^3/min. Previous studies [63,64] used similar generation rate of the same SF_6 source for determining the ventilation effectiveness in indoor spaces that was found to be good.

We measured the air velocity and air temperature in front of the cook at multiple vertical locations. Those measured data could be used to calculate the PD around the cook and the vertical temperature difference between head and feet. The measured SF_6 concentration was used to calculate the capture efficiency through Eq. (5). Fig. 6 shows the kitchen mockup and measurement locations. The capture efficiency of the new ventilation system was calculated by equation (3). Experimental measurements were conducted for summer conditions with an outdoor air temperature of 30.3°C. The temperature from the conditioned air was 23.0°C. The air temperature from infiltration was 29.7°C. The airflow rate listed in Table 1 was used for the experiment.

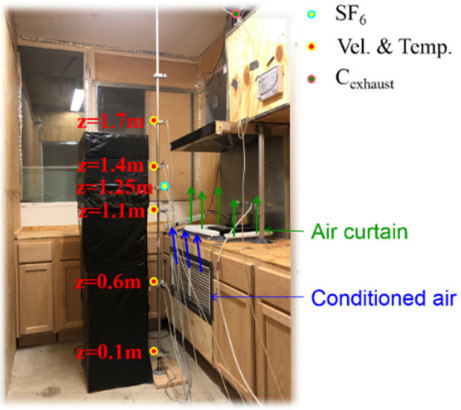

Fig. 6. Kitchen mockup and measurement locations.

3. Results

3.1 Measured thermal comfort and indoor air quality in Chinese residential kitchen

Although all tests were conducted in two consecutive days (September 13 to 14, 2018), outdoor temperature were uncontrollably changing during the test period, ranged from 29.0 to 34.8°C. Different outdoor conditions resulted in different initial indoor environment status of each test. To eliminate the influence of different initial state on thermal comfort, we analyzed all parameters by comparing its relative variation during the test process based on the initial state. Fig. 7 shows a typical case of air temperature distributions in the kitchen as well as the corresponding outdoor air temperature. The indoor air temperature increased, decreased and increased again due to turning on and off the stove for cooking the two dishes. The highest air temperature rise was 6.4°C at the position closest to the stove. The vertical air temperature difference was 5.0°C between P1-0.1m and P1-1.7m and 4.7°C between P2-0.1m and P2-1.7m. The original temperature record for the nine hobo loggers can be found in Appendix 2. Fig. 8 shows the highest air temperature rise during cooking at different measuring locations of the 16 subjects. It also shows the vertical air temperature difference at P1 and P2 of the 16 subjects. The mean median air temperature rise at the "Lower, Middle and Upper" position was 5.3°C. The mean median vertical air temperature difference at P1 and P2 was 3.2°C. The thermal environment in the kitchen was highly non-uniform and too hot, which would cause thermal discomfort.

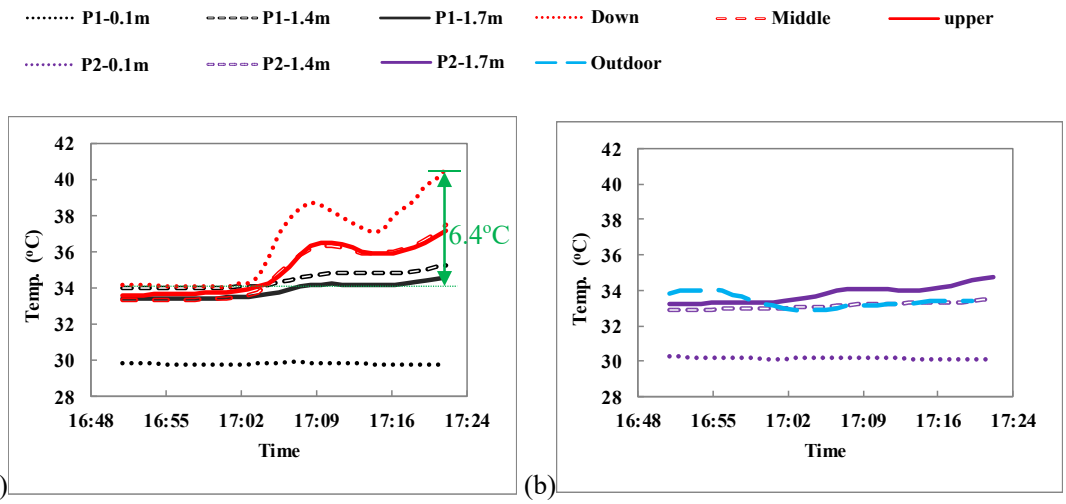

Fig. 7. Field measurement of air temperature changes during cooking in the CRK for a typical subject at: (a) P1, (b) P2 and outdoor.

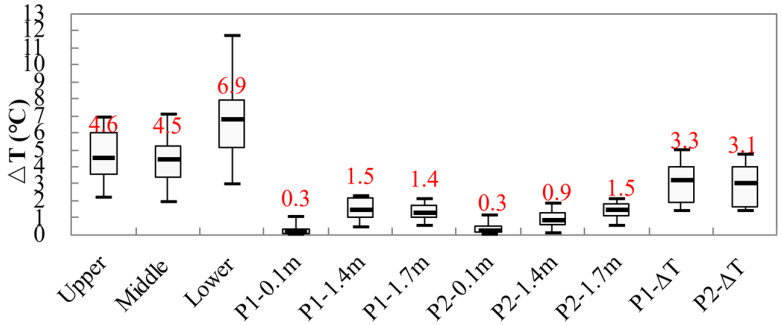

Fig. 8. The highest air temperature rises during the whole cooking period at different measuring locations as well as the vertical air temperature difference at P1 and P2 of the 16 subjects.

Fig. 9 shows the skin temperatures on different body parts and the TSV during cooking for a typical subject. The variation tendency was similar for all subjects. The TSV increased with the skin temperature for the face, thorax, and abdomen regions. However, the skin temperature of the upper leg did not show much difference during cooking since the stove had little influence on it. When the subject turned off the stove, the TSV decreased for one unit. The TSV increased again when the subject turned on the stove. The maximum increase in skin temperature of the four body parts was 3.6, 2.3, 1.8 and 0.1°C, respectively. All the cooks complained that the hottest body parts were the head, face and thorax areas. This was because the three regions were highly exposed to the elevated air and radiant temperatures.

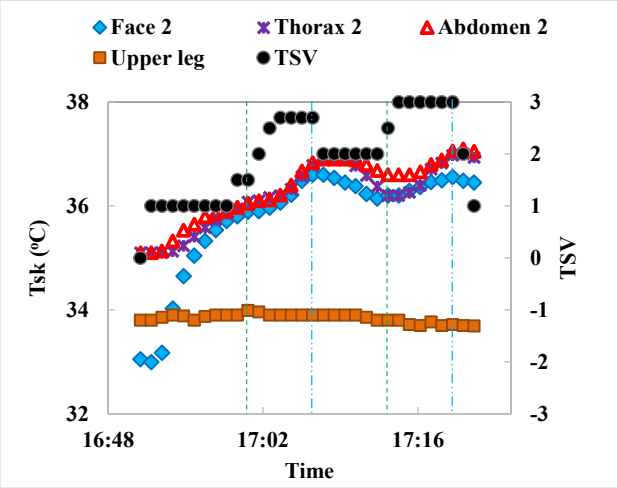

Fig. 9. Skin temperature and the corresponding TSV during cooking for a typical subject for the face, thorax, and abdomen regions. The green and blue dashed line means turning on and off the stove.

Fig. 10 depicts the maximum skin temperature increase on different body parts during the whole cooking period, for the 16 subjects. The skin temperature increase was highest at the head and face region with a median of 3.4°C. The lower body parts and the back were less affected by the stove. The high radiation asymmetry may have distorted the TSV of the subjects. The measured results indicated that the thermal environment in CRKs was too hot in summer. The indoor thermal comfort needs to be improved.

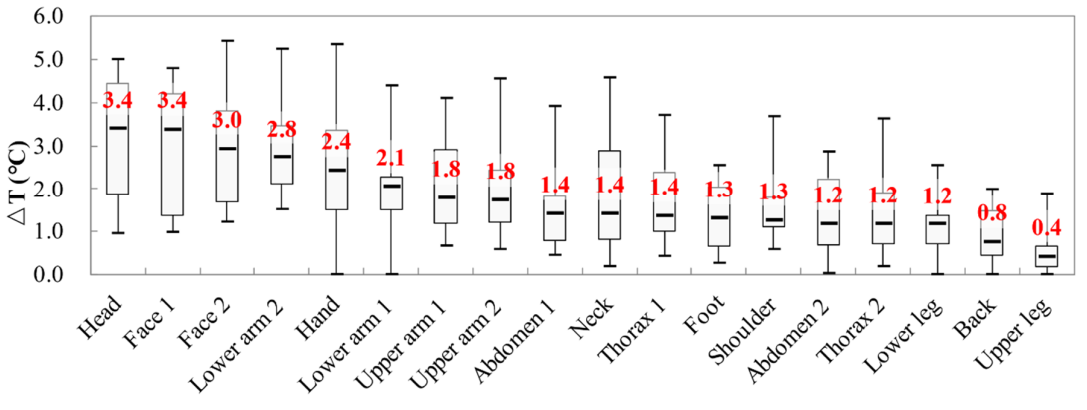

Fig. 10. Skin temperature increase during the whole cooking period on different body parts of the 16 subjects.

Fig. 11 shows the CO, CO_2 and $PM_{2.5}$ concentrations measured at the breathing zone during cooking for a typical subject. Fig. 11(a) illustrates the CO concentration variations during cooking. When the subject turned on the stove, the CO concentration immediately increased to a very high value. The CO concentration then decreased due to the use of exhaust hood. The CO concentration fluctuated during cooking due to frequent changes on gas valve of the stove. It can be concluded that the CO concentration mainly came from the combustion of the natural gas. Fig. 11(b) depicts that the CO_2 concentration gradually increased after the subject entering the kitchen but gradually decreased after the exhaust was on. Fig. 11(c) displays that the $PM_{2.5}$ concentration distribution was bimodal since we asked the subject to cook two dishes in the kitchen. The $PM_{2.5}$ concentration level depends on dish type. The $PM_{2.5}$ concentration exceeded the Chinese standard [14] during the cooking because the ventilation system could not effectively extract the $PM_{2.5}$. We used Tenax TA tubes to measure the TVOC concentration, therefore, only one TVOC concentration was available for each case. The TVOC concentration for this case was 0.64 mg/m^3, which was higher than the limit of the Chinese standard [14].

Fig. 12 shows all the CO, CO_2, TVOC and $PM_{2.5}$ concentrations measured in the kitchen during the whole cooking period for the 16 tests. The red lines indicate the limits of the Chinese national standard GB/T 18883-2002 [14]. The limit of the Chinese standard [14] for TVOCs is an eight-hour average, for CO an hourly average, and for CO_2 a daily average. The measured data for each subject were averaged for the whole cooking period. Then the averaged data for all 16 tests were used to obtain the box plot. Although median value of CO and CO_2 concentrations met the standard, the TOVC and $PM_{2.5}$ concentration exceeded the limit specified by the standards. The indoor air quality was poor.

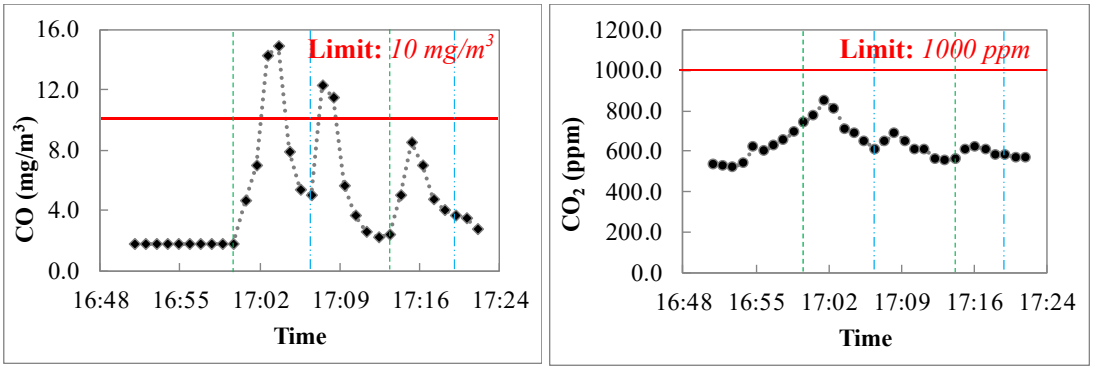

(a)

(b)

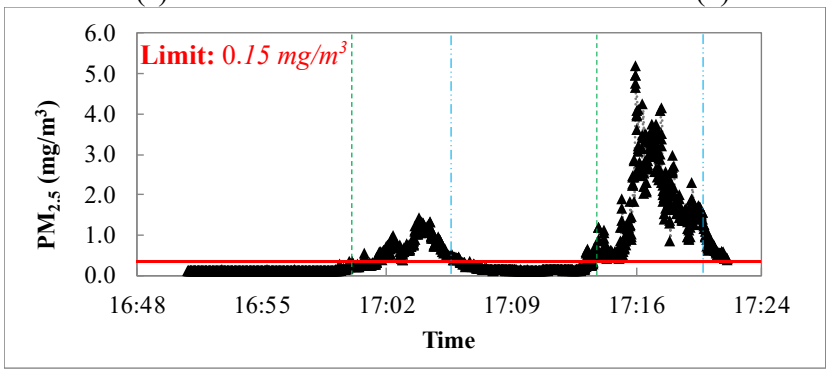

(c)

Fig. 11. Pollutant concentrations, at the breathing zone, measured during the whole cooking period for a typical subject: (a) CO, (b) CO_2, and (c) $PM_{2.5}$. The green and blue dashed line means turning on and off the stove.

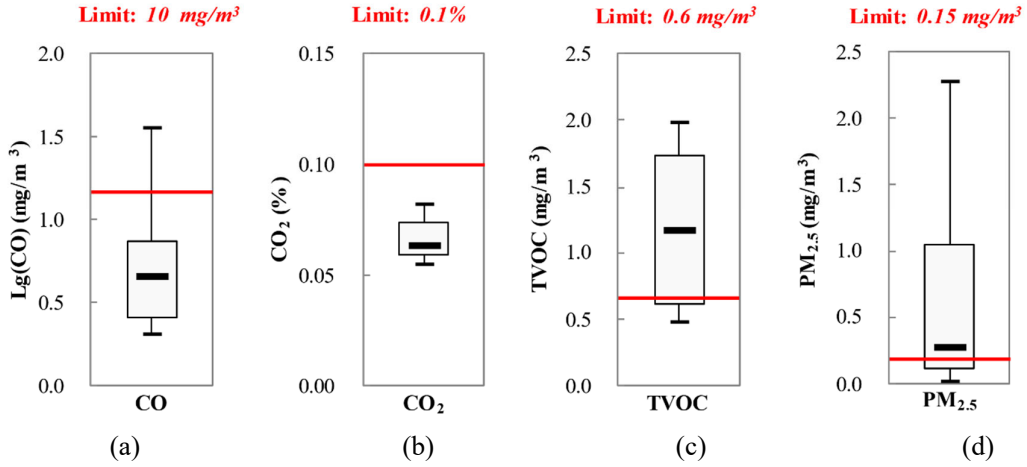

Fig. 12. Pollutant concentrations measured during the whole cooking period for the 16 tests: (a) CO, (b) CO_2, (c) TVOCs, and (d) $PM_{2.5}$.

3.2 New system performance in improving indoor environment in CRKs

Due to the poor thermal environment and air quality in a typical kitchen as shown in the previous section, this investigation proposed a new ventilation system in Section 2.2. This section evaluated the performance of the new ventilation system for summer and winter, respectively.

3.2.1 New system performance in summer conditions

Fig. 13 compares the temperature distribution in the section through the cook and the hood, and the distribution of percentage dissatisfied around the cook, in the summer conditions under different air supply angles from the air conditioner (Cases 1s to 3s of Table 2). We can find that the makeup air from the air curtains mainly centralized in the stove region, which could control the diffusion of the cooking fumes above the stove. It went directly into the exhaust and served as makeup air for the exhaust hood. In addition, the conditioned air was effectively sent into the surrounding of the manikin. At the air supply angles of 45° and 30°, the cold air from the cabinet below the stove would blow directly onto the manikin, which could create strong draft. The maximum draft (PD) values around the cook were 18.4% and 22.0%, respectively, for the two angles. In addition, because the cold air could not reach head level, there were large vertical temperature differences of 6.0 and 5.0°C, respectively. When the air supply angle was 15°, the maximum PD around the manikin decreased to 9.8%, and the vertical temperature difference became -2.2°C. Therefore, Case 3s had the most satisfactory air supply from the air conditioner.

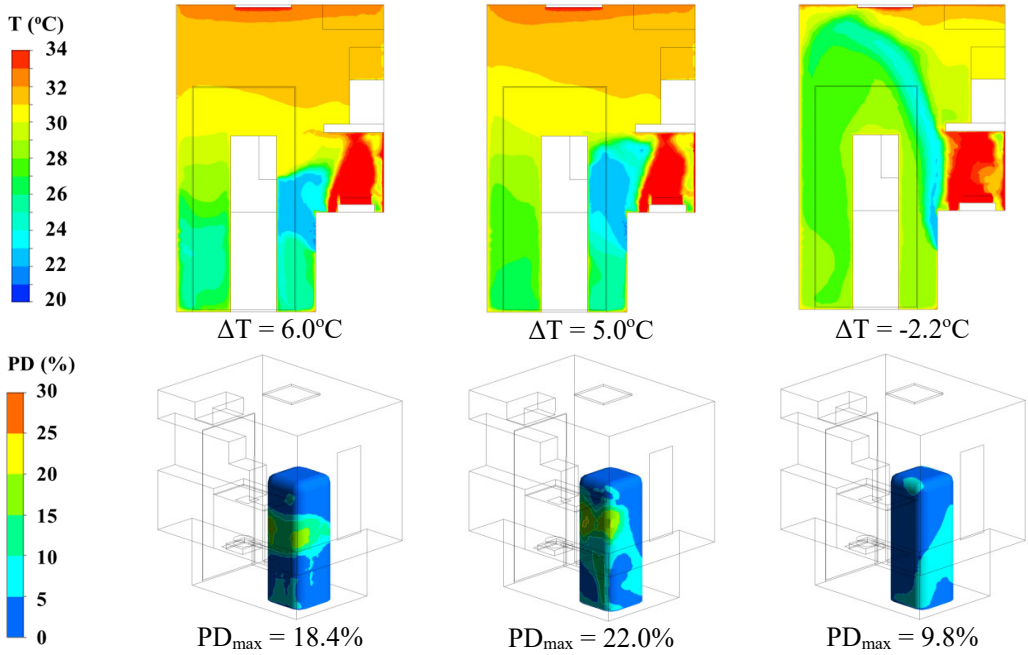

Fig. 13. Numerical predictions of the temperature distribution in the section through the cook and the hood, and the distribution of percentage dissatisfied around the cook, in summer conditions under different air supply angles from the air conditioner: (a) Case 1s, (b) Case 2s, and (c) Case 3s.

With Case 3s as the reference case, Fig. 14 compares the particle deposition on various surfaces in the kitchen at different air supply angles from the air curtains (Cases 3s to 5s). The supply angle from the air curtains had little impact on air quality in the kitchen. The capture efficiency was 96% or higher for all the cases.

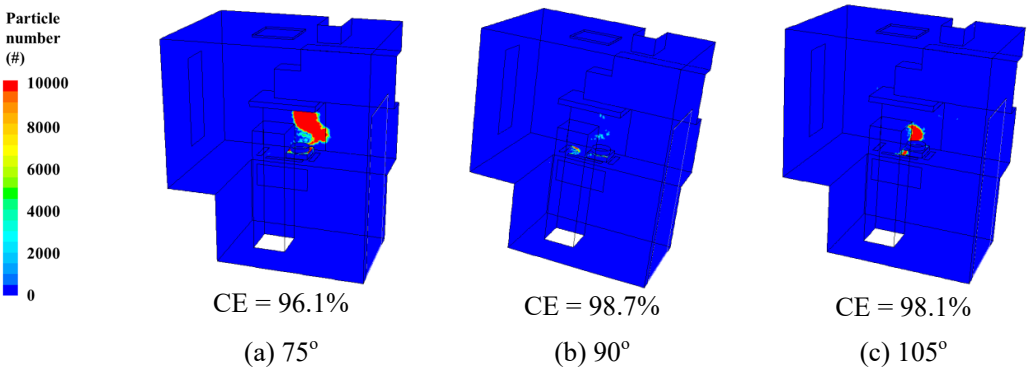

Fig. 14. Particle deposition on various surfaces in the kitchen under different air supply angles from the air curtains in summer: (a) Case 4s, (b) Case 3s, and (c) Case 5s.

By adjusting the air supply opening size, this investigation also evaluated the impact of air supply velocity from the air curtains on capture efficiency (Cases 6s, 3s, and 7s). According to the results, the capture efficiency did not vary greatly with the air curtain velocity. The capture efficiency remained around 98% for all three cases.

3.2.2 New ventilation system performance in winter conditions

Fig. 15 compares the temperature distribution in the section through the cook and hood in the kitchen, and the distribution of percentage dissatisfied around the cook, in the winter conditions under different air supply angles from the air conditioner (Cases 1w to 3w of Table 2). For winter, we used a downward supply because the conditioned air was warmer than the kitchen air. When the air supply angle was 145°, the conditioned air could not reach floor level, which would cause a large vertical temperature difference of 5.9°C. The maximum draft around the manikin was 21.5%. When the air supply angle increased to 155° and 165°, the maximum draft values around the manikin were 22.8% and 31.5% and the vertical air temperature differences were 0.8°C and -0.8°C, respectively. Therefore, Case 2w seemed to be the most satisfactory.

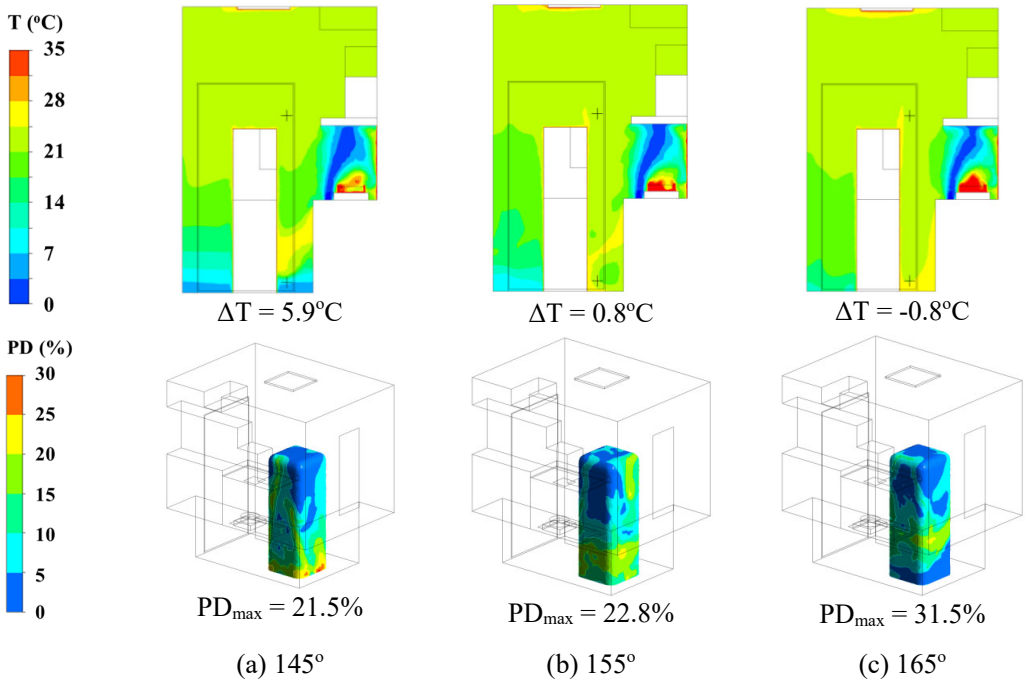

Fig. 15. Numerical predictions of the temperature distribution in the section through the cook and hood in the kitchen, and the distribution of percentage dissatisfied around the cook, in winter conditions under different air supply angles from the air conditioner: (a) Case 1w, (b) Case 2w, and (c) Case 3w.

Next, this investigation compared the influence of supply angle and velocity from the air curtains on the temperature distribution and particle deposition (Cases 4w to 7w). As with the results in summer, the supply angle and velocity from the air curtains had little impact on thermal comfort and air quality in the kitchen in summer condition. The capture efficiency for all the cases was higher than 90%. Fig. 16 compares the numerical predictions of the temperature distribution in kitchen and particle deposition on walls in the kitchen of case 6w, case 2w and case 7w in winter condition. For case 6w, the cold air exhibited a drop off tendency. It means that the momentum of air curtain could not compete with the drop force of the cold air, which would influence the performance of the air curtain. The capture efficiency of this case was 89.7%. When air velocity increased to 1.54 m/s and 2.0 m/s, the CE of both cases became larger than 95%. In addition, for Cases 5w and 7w, the maximum draft around the manikin increased to 34.8% and 42.3%, respectively. This occurred because some cold air from the air curtains escaped from the hood and flowed toward the cook. Therefore, Case 2w

seemed to be the best. Table 3 summarizes the key results (PD_{max}, ΔT and CE) for the new ventilation system. Cases 3s and 2w had the most satisfactory air supply from the air conditioner and air curtains. The proposed ventilation system could maintain good thermal comfort and IAQ in Chinese residential kitchens.

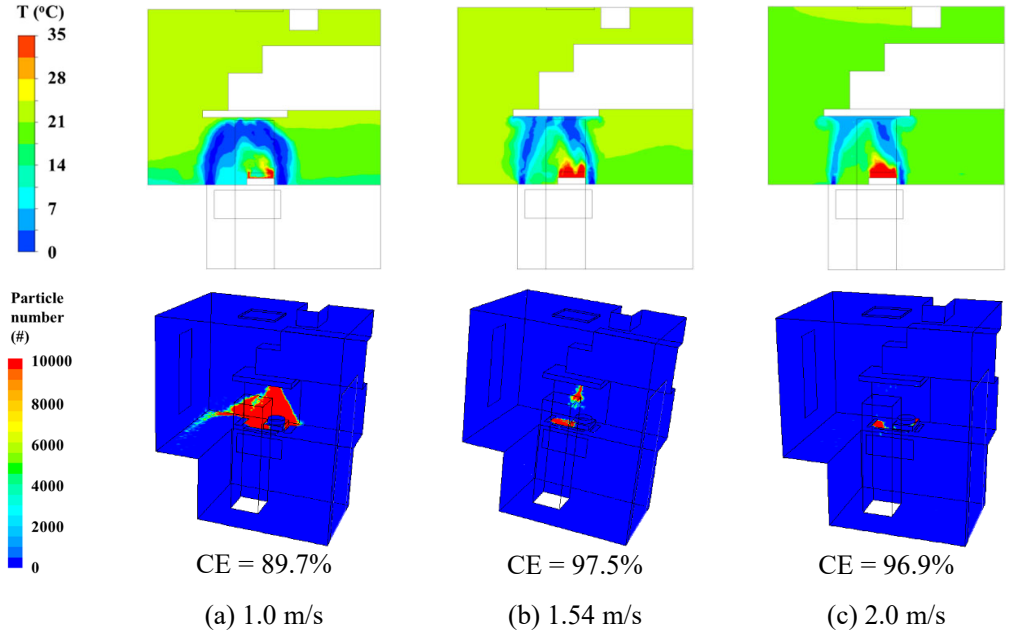

Fig. 16. Numerical predictions of the temperature distribution in kitchen and particle deposition on walls in kitchen in winter condition with different makeup air supply velocities: (a) Case 6w, (b) Case 2w, and (c) Case 7w.

Table 3. Summary of key results for the new ventilation system

Summer				Winter			
Case	PD_{max} (%)	ΔT (°C)	CE (%)	Case	PD_{max} (%)	ΔT (°C)	CE (%)
1s	18.4	6.0	98.3	1w	21.5	5.9	98.4
2s	22.0	5.0	98.5	2w	22.8	0.8	97.5
3s	9.8	-2.2	98.7	3w	31.5	-0.8	98.2
4s	9.9	-1.2	96.1	4w	21.7	-1.1	93.1
5s	8.8	-2.3	98.1	5w	34.8	-5.6	98.2
6s	10.6	-1.7	98.2	6w	21.6	-0.8	89.7
7s	9.8	-2.1	98.2	7w	42.3	-5.5	96.9

3.3 Experimental verification of the new ventilation system performance

To verify our CFD simulation results, experimental measurements with the new ventilation system were conducted in the kitchen mockup at Purdue University, as shown in Fig. 6. Since Case 3s had the best performance, it was used for setting up boundary conditions in the

experiment. Fig. 17 compares the CFD-simulated air velocity, and air temperature profiles in the measurement locations with the measured parameters. The black dots and error bars represent the mean value and standard deviation (SD) of the experimental data. The simulated air velocity and temperature agreed with the measured data in most of the locations. The measured vertical temperature difference between head and feet was -0.9°C. The measured PD in front of the manikin ranged from 3.4% to 19.2%. The SF_6 concentration in the hood outlet was 0.298 ppm with the 0.06 ppm background concentration. The SF_6 concentration in the breathing zone was 0.067 to 0.069 ppm. By using equation (5), the measured capture efficiency was 96.2% to 97.1%. Experimental data shows that proposed ventilation system can maintain good IAQ and thermal environment in CRKs.

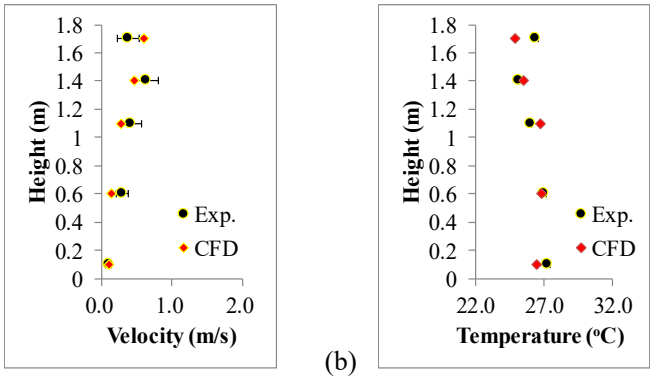

Fig. 17. Experimental data for Case 3s at various measurement locations: (a) velocity, and (b) temperature.

4. Discussion

This investigation compared the proposed ventilation system with the systems of other researchers, as shown in Table 4. Except for Huang et al. [23,24], the other studies all used an air supply angle of 90°. The air supply flow rate in those studies was much lower than that in our system. Therefore, most of the make-up air in the other systems had to come from windows, doors or other leakages. In our system, the air flow rate from the air curtains accounted for 60% of the hood flow rate, and the conditioned air contributed 33%; thus, infiltration was minimal. Therefore, whereas other systems may improve the kitchen environment only slightly, our system provides a capture efficiency of 96%. The proposed ventilation system can solve the problem of thermal discomfort and poor IAQ in CRKs.

Table 4. Comparison of air curtain design for improving thermal comfort and IAQ in CRKs according to different investigations

Ref.	Air curtain schematic	Air curtain details
Huang et al. [23,24]	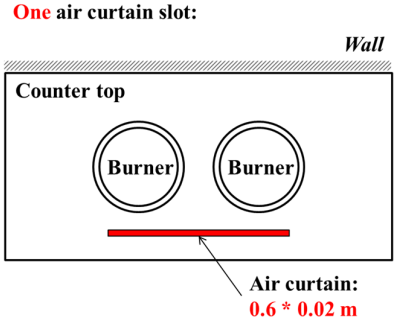	• Upward air curtain • Velocity: 1.0 m/s • Angle: 75° • Flow rate: 41.7 m^3/h • SF_6 spillage: 2 orders of magnitude lower than the baseline case

Zhou et al. [25]	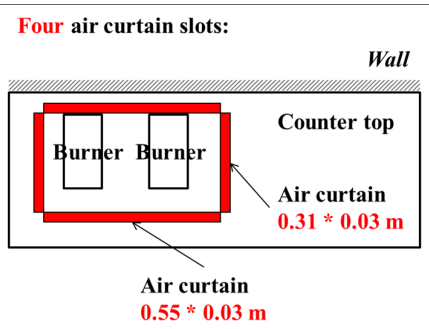	• Upward air curtain • Velocity: 0.5 m/s • Angle: 90° • Flow rate: 92.9 m^3/h • CO_2 reduction efficiency: 23.1%
Zhou et al. [21]	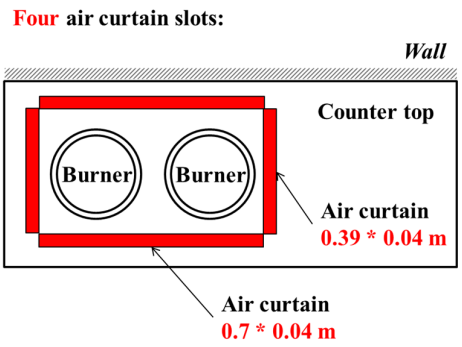	• Upward air curtain • Velocity: 0.5 m/s • Angle: 90° • Flow rate: 157.0 m^3/h • CE: 91.67±3.52 %
Cao et al. [6]	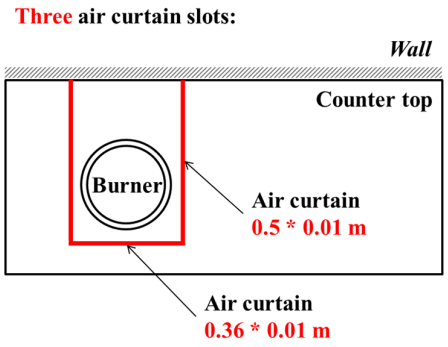	• Upward air curtain • Velocity: 1.0 to 1.5 m/s • Angle: 90° • Flow rate: 49.0 to 73.5 m^3/h • Intake fraction: 1 to 3 orders of magnitude lower than the baseline case
Our investigation	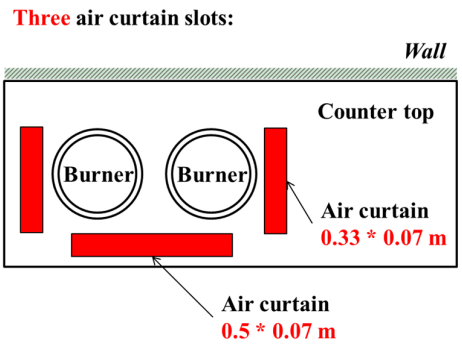	• Upward air curtain • Velocity: 1.54 m/s • Angle: 90° • Flow rate: 450 m^3/h • CE: 96.2%

Meanwhile, this investigation had the following limitations:

- Chinese people prefer stir-frying at home, which accounts for 84.6% of all cooking method [28]. It would be more practical to use real cooking methods such as stir-frying to conduct the CFD simulations. However, it is difficult to measure and calculate parameters of the unsteady stir-frying process.
- This investigation used steady state numerical simulations for the system optimization. However, transient, and non-uniform thermal environment existed in kitchens. The cooking process and pollutant emissions were also unsteady.

- This investigation used SF_6 as tracer gas to measure the capture efficiency of the exhaust hood. However, real cooking processes would release not only gaseous contaminants but also particulate matter of various diameters. The performance of the ventilation system in removing such particulate matter should be further evaluated. It is also important to measure particle deposition on the walls of the kitchen.
- This investigation chosen subjects with an age bias. In addition, follow the same measuring method from previous investigations [2,21,30], this investigation measured the skin temperature by attaching a thermal sensor to the skin with tapes. A few of the measuring points such as head, face, and hand, may exposed to the radiation. It may induce uncertainty.
- This investigation used traditional evaluation method to assess the thermal comfort and air quality in the kitchen. However, there is just a short-term exposure for people in kitchen where the indoor environment was highly non-uniform and transient. The radiation exposure during cooking would affect the thermal comfort. In addition, the cook may exposure to short term high cooking pollutant concentrations. Therefore, the evaluation for thermal comfort and air quality should be different from long-term stay space like living room or bedroom. Zhou et al. [10] used four thermal comfort models, including PMV [9], the dynamic thermal sensation model (DTS) from Fiala [65], the University of California at Berkeley (UCB) model [66], and the dynamic outdoor thermal comfort model from Lai's [67], to predict the individual thermal sensation in a CRK and compared with the actual TSV. They found that none of the models provided acceptable results. A transient and non-uniform thermal comfort model should be developed for evaluate the thermal comfort in the CRKs. In addition, it is important to explore the unsteady exposure of the cooking pollutants during cooking and define the corresponding health risk.
- Generally, three types of air conditioners could be used in CRKs: wall-mounted, ceiling-mounted, and movable air-conditioner. Without using a makeup air system, the supply air from the conditioner may disturb the air distribution around stove, and thus decrease the capture efficiency of exhaust hood. In addition, the conditioned air in the kitchen was discharged directly to outdoor environment by the exhaust hood, which would lead to energy waste. Such system could not prevent cooking fume from entering the kitchen air so particles could deposit on walls and other kitchen surfaces. Our proposed ventilation system would prevent such problems and is more energy efficient.
- Although the proposed ventilation system seems complicated for residential kitchens. Makeup air and air-conditioning systems have been widely used in commercial kitchens. By migrating the concept from commercial kitchens to residential kitchens, it is beneficial to improve indoor air quality and thermal comfort for CRKs for the well beings of building occupants.
- Zhou et al. [21] found that the capture efficiency of the exhaust hood when opening window with using air curtains was around 10% higher than that when closing window. The airflow rate from the air curtains was 157.0 m^3/h (31.4% of the exhaust flow rate). The airflow rate from the air curtains in our proposed system was 450 m^3/h (60% of the exhaust flow rate). Therefore, opening window or door would not jeopardize the performance of the air curtains in our system. In shoulder season when outdoor temperature and air quality is favorable, one could open the window and use air curtains to provide the makeup air needed.
- In our experiment, we have a control system which could control the air flow rate from the conditioned air and make-up air. In actual application, one can use fan and constant air volume regulating valve to control the flow rate needed. In addition, most industrial, commercial, and institutional buildings of any size incorporate mechanical systems for

the supply and distribution of fresh air which may be filtered, heated, or cooled, and humidified, as required [68]. To avoid the microbial pollution in the duct work, additional filtration systems may also be used to control air quality by the removal of atmospheric contamination from outdoors and ductwork.

5. Conclusions

This investigation measure thermal comfort and indoor air quality for a Chinese residential kitchen. Then proposed an integrated air-curtain and air-conditioning system to improve the thermal environment and indoor air quality in Chinese residential kitchens. CFD simulations were performed to optimize the design parameters for both summer and winter conditions. The study led to the following conclusions:

- The thermal environment in the Chinese residential kitchen was highly non-uniform and too hot in summer. The air temperature could increase 5.3°C for cooking two dishes in a typical kitchen. The vertical air temperature difference was 3.2°C. The measured TVOCs and $PM_{2.5}$ concentrations exceeded the limits set by the Chinese national standard.
- The new system supplied conditioned air from the lower part of the cabinet under the cooking stove, and make-up air from the air curtains around the stove. The airflow rate from the air curtains accounted for 60% of the hood flow rate, and the conditioned air contributed 33%. When the airflow rate of the exhaust hood was 750 m^3/h, the optimal air supply angle for the air curtains was 90° and the air velocity 1.5 m/s.
- Experimental measurements were conducted in a kitchen mockup to verify the performance of the new system. The measured capture efficiency was 96.2% to 97.1%, PD around the cook lower than 20%, and vertical temperature difference between head and feet -0.9°C. The proposed ventilation system could maintain good IAQ and thermal comfort for CRKs.

Acknowledgement

The research presented in this paper was partially supported by the National Key R&D Program of the Ministry of Science and Technology, China, on “Green Buildings and Building Industrialization” through Grant No. 2016YFC0700500 and by the National Natural Science Foundation of China through Grant No. 51678395.

References

[1] Lai C. Assessment of side exhaust systems for residential kitchens in Taiwan. Building Services Engineering Research and Technology, 2005, 26(2): 157-166.
[2] Wei P, Zhou B, Tan M, et al. Study on thermal comfort under non-uniform thermal environment condition in domestic kitchen. Procedia Engineering, 2017, 205: 2041-2048.
[3] Kim C, Gao Y T, Xiang Y B, et al. Home kitchen ventilation, cooking fuels, and lung cancer risk in a prospective cohort of never smoking women in Shanghai, China. International Journal of Cancer, 2015, 136(3): 632-638.
[4] Hou J, Sun H, Zhou Y, et al. Environmental exposure to polycyclic aromatic hydrocarbons, kitchen ventilation, fractional exhaled nitric oxide, and risk of diabetes among Chinese females. Indoor air, 2018, 28(3): 383-393.
[5] Dai W, Zhong H, Li L, et al. Characterization and health risk assessment of airborne pollutants in commercial restaurants in northwestern China: under a low ventilation condition in wintertime. Science of the Total Environment, 2018, 633: 308-316.
[6] Cao C, Gao J, Wu L, et al. Ventilation improvement for reducing individual exposure to cooking-generated particles in Chinese residential kitchen. Indoor and Built Environment, 2017, 26(2): 226-237.
[7] Yik F W H, Sat P S K, Niu J L. Moisture generation through Chinese household activities. Indoor and built environment, 2004, 13(2): 115-131.
[8] Liu S, Dong J, Cao Q, et al. Indoor thermal environment and air quality in Chinese‐style residential kitchens. Indoor Air, 2019, doi.org/10.1111/ina.12631.
[9] ASHRAE Standard 55-2010: Thermal environmental conditions for human occupancy. ASHRAE, Atlanta USA, 2010.
[10] Zhou X., Liu S. Liu X, et al. Evaluation of four models for predicting thermal sensation in Chinese residential kitchen. CLIMA 2019, May 26-29, 2019, Bucharest, Romania.
[11] Wang H, Xiang Z, Wang L, et al. Emissions of volatile organic compounds (VOCs) from cooking and their speciation: A case study for Shanghai with implications for China. Science of the Total Environment, 2018, 621: 1300-1309.
[12] Liu L. 2007. Detection and evaluation of air pollution in kitchen. Gas & Heat, 2007, 5.
[13] Du B, Gao J, Chen J, et al. Particle exposure level and potential health risks of domestic Chinese cooking. Building and Environment, 2017, 123: 564-574.
[14] GB/T 18883-2002. Indoor air quality standard. Beijing: Standardization Administration of China, 2002.
[15] Zhao Y, Li A, Gao R, et al. Measurement of temperature, relative humidity and concentrations of CO, CO_2 and TVOC during cooking typical Chinese dishes. Energy and Buildings, 2014, 69: 544-561.
[16] Zhou J, Zhao Y. Residential kitchen smoke pollution field tests and numerical simulation. Contamination Control & Air-conditioning Technology, 2015, 2.
[17] See SW, Balasubramanian R. Physical characteristics of ultrafine particles emitted from different gas cooking methods. Aerosol and Air Quality Research, 2006, 6(1): 82-92.
[18] Zhao Y, Hu M, Slanina S, et al. Chemical compositions of fine particulate organic matter emitted from Chinese cooking. Environmental Science & Technology, 2007, 41(1): 99-105.
[19] GB/T 17713-2011. Range hood. Beijing: Standardization Administration of China, 2011.
[20] Liu J, Dai X, Li X, etc. Indoor air quality and occupants' ventilation habits in China: Seasonal measurement and long-term monitoring. Building and Environment, 2018, 142: 119-129.
[21] Zhou B, Wei P, Tan M, et al. Capture efficiency and thermal comfort in Chinese residential kitchen with push-pull ventilation system in winter-A field study. Building and Environment, 2019, 149: 182-195.
[22] Liu X, Wang X, Xi G. Orthogonal design on range hood with air curtain and its effects on kitchen environment. Journal of Occupational and Environmental Hygiene, 2014, 11(3): 186-199.
[23] Huang R F, Nian Y C, Chen J K. Static condition differences in conventional and inclined air-curtain range hood flow and spillage characteristics. Environmental Engineering Science, 2010, 27(6): 513-522.
[24] Huang R F, Nian Y C, Chen J K, et al. Improving flow and spillage characteristics of range hoods by using an inclined air-curtain technique. Annals of Occupational Hygiene, 2010, 55(2): 164-179.
[25] Zhou B, Chen F, Dong Z, et al. Study on pollution control in residential kitchen based on the push-pull ventilation system. Building and Environment, 2016, 107: 99-112.
[26] Livchak A, Schrock D, Sun Z. The effect of supply air systems on kitchen thermal environment. ASHRAE Transactions, 2005, 111(1): 748-754.

[27] Huang R F, Dai G Z, Chen J K. Effects of mannequin and walk-by motion on flow and spillage characteristics of wall-mounted and jet-isolated range hoods. Annals of Occupational Hygiene, 2010, 54(6): 625-639.
[28] Chen C, Zhao Y, Zhao B. Emission rates of multiple air pollutants generated from Chinese residential cooking. Environmental science & technology, 2018, 52(3): 1081-1087.
[29] Zhao Y, Zhao B. Emissions of air pollutants from Chinese cooking: A literature review. Building simulation. Tsinghua University Press, 2018, 11(5): 977-995.
[30] Lai D, Zhou X, Chen Q. Measurements and predictions of the skin temperature of human subjects on outdoor environment. Energy and Buildings, 2017, 151: 476-486.
[31] Zhou X, Lai D, Chen Q. Experimental investigation of thermal comfort in a passenger car under driving conditions. Building and environment, 2019, 149: 109-119.
[32] Deng Q, Wang R, Li Y, et al. Human thermal sensation and comfort in a non-uniform environment with personalized heating. Science of the Total Environment, 2017, 578: 242-248.
[33] Melikov A K. Personalized ventilation. Indoor air, 2004, 14: 157-167.
[34] Amai H, Tanabe S, Akimoto T, et al. Thermal sensation and comfort with different task conditioning systems. Building and Environment, 2007, 42(12): 3955-3964.
[35] Pan D, Deng S, Chan M. Optimization on the performances of a novel bed-based task/ambient conditioning (TAC) system. Energy and Buildings, 2017, 144: 181-190.
[36] Zhang Y, Zhao R. Relationship between thermal sensation and comfort in non-uniform and dynamic environments. Building and Environment, 2009, 44(7): 1386-1391.
[37] Liu S, Dong J, Cao Q, et al. Indoor thermal environment and air quality in Chinese-style residential kitchens. Indoor Air, 2019.
[38] P.O. Fanger, A.K. Melikov, H. Hanzawa, et al. Air turbulence and sensation of draught. Energy and Buildings, 1988, 12(1): 21-39.
[39] Ellenbecker M J, Gempel R F, Burgess W A. Capture efficiency of local exhaust ventilation systems. American Industrial Hygiene Association Journal, 1983, 44(10): 752-755.
[40] Li Y C, Shu M, Ho S S H, et al. Characteristics of $PM_{2.5}$ emitted from different cooking activities in China. Atmospheric Research, 2015, 166: 83-91.
[41] Guo M, Xing R, Shimada Y, et al. Individual exposure to particulate matter in urban and rural Chinese households: Estimation of exposure concentrations in indoor and outdoor environments. Natural Hazards, 2019: 1-18.
[42] GB/T 50096-2011. Design code for residential buildings. Beijing: Standardization Administration of China, 2002.
[43] Gao N, Niu J. CFD study on micro-environment around human body and personalized ventilation. Building and Environment, 2004, 39(7): 795-805.
[44] Liu Y, Li H, Feng G. Simulation of inhalable aerosol particle distribution generated from cooking by Eulerian approach with RNG k–epsilon turbulence model and pollution exposure in a residential kitchen space. Building Simulation. Tsinghua University Press, 2017, 10(1): 135-144.
[45] ANSYS Inc.. ANSYS Fluent 14.0 User's Guide. ANSYS Inc. Southpointe. 2011.
[46] Shih T H, Liou W W, Shabbir A, et al. A new k-ε eddy viscosity model for high Reynolds number turbulent flows. Computers & Fluids, 1995, 24(3): 227-238.
[47] Zhao B, Zhang Y, Li X, et al. Comparison of indoor aerosol particle concentration and deposition in different ventilated rooms by numerical method. Building and Environment, 2004, 39(1): 1-8.
[48] Li A, Ahmadi G. Dispersion and deposition of spherical particles from point sources in a turbulent channel flow. Aerosol science and technology, 1992, 16(4): 209-226.
[49] Zhang H, Wang F, Wang Y, et al. CFD Simulation of Cooking Particle Distribution and Motion. Procedia Engineering, 2017, 205: 1800-1806.
[50] Elghobashi S. On predicting particle-laden turbulent flows. Applied scientific research, 1994, 52(4): 309-329.
[51] Chen C, Lin C H, Wei D, et al. Modeling particle deposition on the surfaces around a multi-slot diffuser. Building and Environment, 2016, 107: 79-89.
[52] GAMBIT CFD Preprocessor. User's Guide. Lebanon, NH: Fluent Inc. 1998.
[53] Ai Z, Mak C M, Gao N, et al. Tracer gas is a suitable surrogate of exhaled droplet nuclei for studying airborne transmission in the built environment. Building Simulation. Tsinghua University Press, 2020: 1-8.
[54] Zhang Z, Chen X, Mazumdar S, et al. Experimental and numerical investigation of airflow and contaminant transport in an airliner cabin mockup. Building and Environment, 2009, 44(1): 85-94.

[55] Li F, Liu J, Pei J, et al. Experimental study of gaseous and particulate contaminants distribution in an aircraft cabin. Atmospheric Environment, 2014, 85: 223-233.
[56] Tang J W, Noakes C J, Nielsen P V, et al. Observing and quantifying airflows in the infection control of aerosol-and airborne-transmitted diseases: an overview of approaches. Journal of Hospital Infection, 2011, 77(3): 213-222.
[57] Noakes C J, Fletcher L A, Sleigh P A, et al. Comparison of tracer techniques for evaluating the behaviour of bioaerosols in hospital isolation rooms. Proceedings of healthy buildings. 2009: 13-17.
[58] Bivolarova M, Ondráček J, Melikov A, et al. A comparison between tracer gas and aerosol particles distribution indoors: The impact of ventilation rate, interaction of airflows, and presence of objects. Indoor Air, 2017, 27(6): 1201-1212.
[59] ASTM International. 2017. ASTM E3087-17. Standard Test Method for Measuring Capture Efficiency of Domestic Range Hoods.
[60] Kim Y S, Walker I S, Delp W W. Development of a standard capture efficiency test method for residential kitchen ventilation. Science and Technology for the Built Environment, 2018, 24(2): 176-187.
[61] LumaSense Technologies. (2017). INNOVA 1309 User Manual. Retrieved from. https://innova.lumasenseinc.com/manuals/historical-manuals/1309/
[62] LumaSense Technologies. (2017). INNOVA 1312 User Manual. Retrieved from https://innova.lumasenseinc.com/manuals/historical-manuals/1312/
[63] Lau J, Chen Q. Floor-supply displacement ventilation for workshops. Building and Environment, 2007, 42(4): 1718-1730.
[64] Shi Z, Lu Z, Chen Q. Indoor airflow and contaminant transport in a room with coupled displacement ventilation and passive-chilled-beam systems. Building and Environment, 2019, 161: 106244.
[65] Fiala D, Havenith G, Bröde P, et al. UTCI-Fiala multi-node model of human heat transfer and temperature regulation. International Journal of Biometeorology, 2012, 56(3): 429-441.
[66] Zhang H, Arens E, Huizenga C, et al. Thermal sensation and comfort models for non-uniform and transient environments, Part III: Whole-body sensation and comfort. Building and Environment, 2010, 45(2): 399-410.
[67] Lai D, Zhou X, Chen Q. Modelling dynamic thermal sensation of human subjects in outdoor environments. Energy and Buildings, 2017, 149: 16-25.
[68] Brief R S, Bernath T. Indoor pollution: Guidelines for prevention and control of microbiological respiratory hazards associated with air conditioning and ventilation systems. Applied Industrial Hygiene, 1988, 3(1): 5-10.

Appendix 1: Grid independence analysis

Fig. 1 compares the computed air velocity and temperature in front of the cook obtained from the three grids. The position of the line was in accordance with the measuring line shown in the kitchen mockup. It can be found that the grid number of 1.4 million provided grid-independent results. Fig. 2 shows the grid size for 1.4 million cells ranged from 0.01 to 0.03 m, depending on the geometric requirements. The average wall y+ was 18, and thus the standard wall functions could be used.

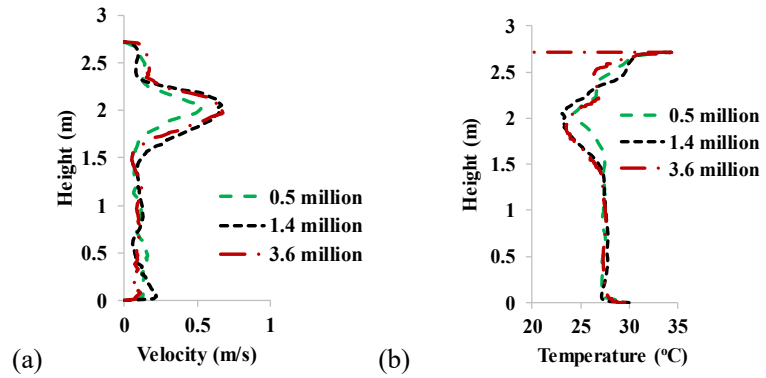

Fig. 1. Simulated results by different grids for: (a) air velocity and (b) air temperature.

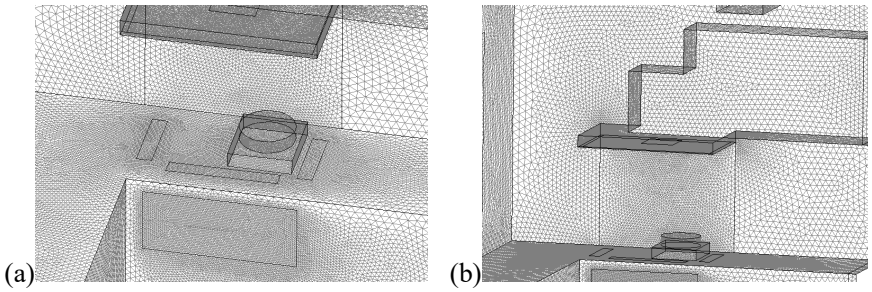

Fig. 2. Grid distribution for (a) the stove region and (b) the exhaust hood region.

Appendix 2: The original temperature record for the nine hobo loggers of the typical case.

Time	P1-0.1m	P1-1.4m	P1-1.7m	P2-0.1m	P2-1.4m	P2-1.7m	Upper	Middle	Lower
16:51:01	29.9	34.0	33.4	30.3	32.9	33.2	33.5	33.3	34.2
16:52:01	29.8	34.0	33.4	30.3	32.9	33.3	33.5	33.3	34.2
16:53:01	29.8	34.0	33.4	30.2	32.9	33.3	33.6	33.3	34.2
16:54:01	29.8	34.0	33.4	30.2	32.9	33.3	33.6	33.3	34.2
16:55:01	29.8	34.0	33.4	30.2	32.9	33.3	33.6	33.3	34.1
16:56:01	29.8	34.0	33.4	30.2	33.0	33.3	33.6	33.3	34.1
16:57:01	29.8	34.0	33.4	30.2	33.0	33.3	33.6	33.3	34.1
16:58:01	29.7	34.0	33.4	30.2	33.0	33.3	33.7	33.3	34.1
16:59:01	29.7	34.0	33.4	30.2	33.0	33.3	33.7	33.4	34.1
17:00:01	29.7	34.0	33.4	30.2	33.0	33.3	33.7	33.4	34.0
17:01:01	29.7	34.0	33.5	30.1	33.0	33.4	33.7	33.4	34.0
17:02:01	29.7	34.1	33.5	30.2	33.0	33.4	33.8	33.5	34.2
17:03:01	29.8	34.1	33.5	30.2	33.0	33.4	33.9	33.6	34.3
17:04:01	29.8	34.1	33.6	30.2	33.0	33.5	34.0	33.8	34.6
17:05:01	29.8	34.2	33.6	30.2	33.1	33.7	34.3	34.2	35.7
17:06:01	29.9	34.3	33.8	30.2	33.1	33.8	34.6	34.8	37.0
17:07:01	29.9	34.4	33.9	30.2	33.1	34.0	35.2	35.3	37.8
17:08:01	29.9	34.6	34.0	30.2	33.2	34.0	35.8	35.8	38.4
17:09:01	29.9	34.7	34.1	30.2	33.2	34.1	36.3	36.2	38.8
17:10:01	29.9	34.7	34.2	30.2	33.2	34.1	36.5	36.3	38.6

17:11:01	29.9	34.8	34.2	30.2	33.3	34.1	36.5	36.3	38.2
17:12:01	29.8	34.8	34.2	30.2	33.3	34.1	36.4	36.2	37.9
17:13:01	29.8	34.8	34.2	30.2	33.3	34.0	36.2	36.1	37.6
17:14:01	29.8	34.8	34.1	30.2	33.3	34.0	36.0	35.9	37.3
17:15:01	29.8	34.8	34.1	30.1	33.3	34.0	35.9	35.9	37.1
17:16:01	29.8	34.8	34.1	30.1	33.3	34.1	35.9	36.0	37.1
17:17:01	29.8	34.8	34.2	30.1	33.3	34.2	35.9	36.0	38.0
17:18:01	29.8	34.9	34.3	30.1	33.3	34.3	36.1	36.2	38.4
17:19:01	29.8	34.9	34.3	30.1	33.4	34.4	36.3	36.3	38.8
17:20:01	29.8	35.0	34.4	30.1	33.4	34.5	36.5	36.6	39.7
17:21:01	29.8	35.1	34.5	30.1	33.4	34.7	36.8	37.0	40.0
17:22:01	29.8	35.2	34.6	30.1	33.5	34.8	37.2	37.5	40.5